Reactions of Laser-Ablated V, Cr, and Mn Atoms with Nitrogen Atoms and Molecules. Infrared Spectra and Density Functional Calculations on Metal Nitrides and Dinitrogen Complexes

Lester Andrews,* William D. Bare, and George V. Chertihin

Department of Chemistry, University of Virginia, Charlottesville, Virginia 22901

Received: May 29, 1997[⊗]

Laser-ablated V, Cr, and Mn atoms mixed with Ar/N_2 and pure N_2 during condensation at 6−10 K produced and trapped the VN, CrN, and MnN molecules and their dinitrogen complexes. The M−N vibrations were characterized by nitrogen 14/15 isotopic ratios. Stepwise annealing converted the MN molecules into $(NN)_xMN$ complexes. The NCrN molecule was identified from nitrogen-14,15 and chromium-52,53,54 isotopic spectra. In addition to end-bonded $M(NN)_x$ complexes in the 2200−1900 cm^{-1} region, evidence for side-bonded $M(N_2)$ complexes was found in the 1900−1700 cm^{-1} region. Density functional calculations provide support for the vibrational assignments.

Introduction

In the solid phase, interstitial nitrogen greatly increases the yield strength of stainless steel alloys containing chromium, nickel, and manganese, which is due in part to the presence of interstitial nitrides.[1] Furthermore, high nitrogen chromium−manganese stainless steels at elevated temperatures show a precipitation of Cr_2N particles.[2] The effect of nitride-forming transition metals on nitrogen solubility in iron melts has been investigated.[3] Nitride-forming elements such as vanadium and chromium create hard, wear-resistant coatings for tools.[4] Clearly, nitrogen and transition metal atoms interact strongly in the solid phase, and interstitial nitrides are important in stainless steel alloys. Transition metal nitrides, in particular vanadium nitride, are also used as new catalysts for hydroprocessing.[5]

In the gas phase, transition metal nitrides are challenging subject molecules for experiment and theory, and as a result, relatively little work has been done on these systems. Vibrational fundamentals are known only for TiN (1039.6 cm^{-1}) and VN (1020 ± 5 cm^{-1}) in the gas phase,[6,7] FeN (938.0 cm^{-1}) and CoN (826.5 cm^{-1}) in solid argon, and NiN (838.8 cm^{-1}) in solid nitrogen.[8,9] Detailed multiconfiguration self-consistent field (MCSCF) and multireference configuration interaction (MRCI) ab initio calculations on the ScN, TiN, VN, and CrN series have described the ground states as triple bonded with the remaining valence electrons essentially localized on the transition metal.[10,11] Although TiN has been studied extensively in the gas phase[6,12−16] and by theory,[11,17,18] VN has been observed in emission,[7] the only experimental measurement on CrN is the dissociation energy,[19] and we have found no reports on investigation of the MnN molecule.

Pulsed-laser ablation of transition metal targets provides an effective way to make the metal nitrides, since molecular nitrogen can be dissociated by the energetic metal atoms produced by laser ablation. In this manner, both FeN and NFeN were observed and trapped in solid argon and nitrogen for matrix infrared spectroscopic study, and both ^{15}N substitution and ^{54}Fe, ^{56}Fe isotopes in natural abundance and density functional theory (DFT) calculations were employed to characterize these species.[8] Experiments with Co and Ni gave CoN and NiN and the rhombic dimer molecules $(CoN)_2$ and $(NiN)_2$ with evidence of metal−metal bonding across the rhombic rings.[9]

We report here similar studies on the laser-ablated V−, Cr− and Mn−nitrogen systems. In addition to nitrides, dinitrogen complexes are also produced for each metal. Such complexes have been reported for chromium[20,21] and vanadium[22] but not for manganese. Side-bonded $M(N_2)$ complexes with substantially reduced N−N stretching frequencies are of particular interest for nitrogen fixation processes.

Experimental Section

The laser ablation and matrix infrared methods have been described;[8,23−25] higher energy (40−90 mJ) laser pulses were employed here. Vanadium, chromium, and manganese targets (Johnson Matthey) and isotopic nitrogen (99 and 53% ^{15}N, Isotec, Inc.) were used as received. Argon mixtures with 1−4% nitrogen, as well as pure nitrogen, were reacted with metal atoms. Several experiments employed microwave discharge during deposition to randomize isotopic mixtures. Laser-ablated metal atoms were codeposited with gas mixtures for 1 h on a CsI window embedded in a copper block cooled to 10 ± 1 K. Infrared spectra were recorded, samples were sequentially annealed and quenched, and more spectra were recorded. Annealing temperatures were measured by a thermocouple attached to the copper block and by residual argon or nitrogen vapor pressure.

Results

Fourier transform infrared (FTIR) spectra will be reported for vanadium, chromium, and manganese atoms codeposited with Ar/N_2 and pure nitrogen samples.

V + Ar/N_2. Laser-ablated V atoms were codeposited with 2% N_2 in argon, the 2300−1600 cm^{-1} region is shown in Figure 1, and the new product absorptions are listed in Table 1. Note the evolution of bands as the sample is subsequently annealed to 25, 35, and 40 K and quenched to 10 K (Figure 1b−d). New sharp weak bands were also observed at 1026.2, 1020.3, and 1014.4 cm^{-1}, which gave way on annealing to a 997.8 cm^{-1} absorption. Weak bands also appeared between 563 and 468 cm^{-1} on annealing. Similar spectra were obtained using $^{15}N_2$, and the bands were shifted as given in Table 1.

Four experiments were done with $^{14}N_2 + {}^{15}N_2$ mixtures. A 2% $^{14}N_2$ + 2% $^{15}N_2$ sample was reacted with laser-ablated V

[⊗] Abstract published in *Advance ACS Abstracts,* October 1, 1997.

S1089-5639(97)01721-0 CCC: $14.00

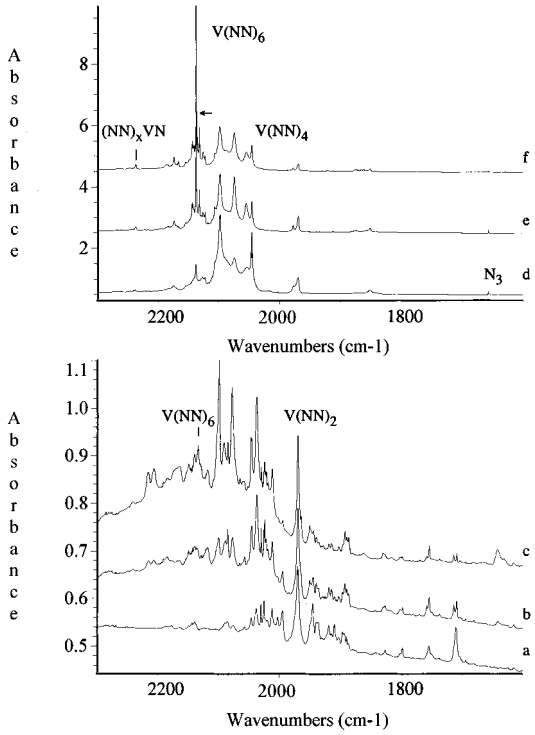

Figure 1. Infrared spectra in the 2300−1600 cm^{-1} region for laser-ablated V atoms codeposited with nitrogen at 10 ± 1 K. (a) 2% N_2 in argon codeposited for 1.5 h, (b) after annealing to 25 K, (c) after annealing to 35 K, (d) pure nitrogen codeposited for 1 h, (e) after annealing to 25 K, arrow denotes peak of 2137.7 cm^{-1} band, and (f) after annealing to 35 K on thermocouple temperature indicator.

atoms, and this experiment was repeated subjecting the gas mixture to microwave discharge (40 W nominal) prior to reaction with metal atoms; spectra in the 1040−960 cm^{-1} region were identical except the product band intensity was greater and noise was higher in the discharge experiment. Spectra from the former experiment are shown in Figure 2. A very weak VO_2 band (A = 0.003) at 935.9 cm^{-1} (not shown) indicates that little oxide contamination was present.[23] Four very weak bands (A = 0.002−0.001) were observed at 1026.2, 1010.3, 1014.4, and 1010.6 cm^{-1} from nitrogen-14 with an identical set at 999.4, 993.6, 987.9, and 984.2 cm^{-1} from nitrogen-15 on sample codeposition at 6−7 K (Figure 2a). Annealing to 25 and 30 K slightly decreased the first band and increased the second, third, and fourth bands in each set, increased a 942.0 cm^{-1} band due to $NNVO_2$ complex, and produced new weak bands at 997.8 and 971.4 cm^{-1} (Figure 2b,c). Broad band photolysis decreased the lowest two bands and increased the second band in each set (Figure 2d). Further annealing to 40 K decreased the first three bands, increased a 1002.8 cm^{-1} band (and 976.5 cm^{-1} counterpart) and increased the final 997.8 and 971.4 cm^{-1} bands (Figure 2e). A final annealing to 43 K destroyed the first two bands and increased the last two bands in each set (Figure 2f).

Experiments with 0.5% $^{14}N_2$ + 0.5% $^{15}N_2$ gave weaker bands but a number of differences are of interest. In the upper region, the strongest bands on deposition were 1945.0, 1880.7 and 1709.1, 1657.7 cm^{-1} doublets with a weaker 1970, 1945, 1904 cm^{-1} triplet. Annealing decreased these bands and produced a 1641.4, 1568.8 cm^{-1} doublet, a sharp 2078, 2009 cm^{-1} doublet, and a broad 2209, 2134 cm^{-1} doublet with weak 2174, 2156 cm^{-1} intermediate bands. When these samples were discharged to render the isotopic mixture statistical, the 1970 cm^{-1} band became a sextet and the 1709.1 and 1641.4 cm^{-1} bands became triplets. In the lower region, the first band, 1026.2 and 999.4 cm^{-1}, in each isotopic set was about 3 times stronger than the second member, and annealing to 25 and 30 K reversed this relationship. Weaker third, fourth, and fifth bands were observed, and annealing to 40 K removed the first band, the second band was the strongest, and the final band was the weakest member of the set.

TABLE 1: Infrared Absorptions (cm^{-1}) from Codeposition of Laser-Ablated Vanadium Atoms with 2% N_2 in Argon at 10 ± 1 K

$^{14}N_2$	$^{15}N_2$	R(14/15)	anneal[a]	assign
2237 w	2162	1.0347	+	$(NN)_xVN$
2215.6	2142.1	1.0343	++	?
2206.7	2133.9	1.0341	++	?
2164.6	2093.3	1.0341	+	?
2140.1	2069.0	1.0344	+	$V(NN)_6$
2133.9	2065.3	1.0332	+	$V(NN)_6$
2098.9	2031.3	1.0333	+	$V(NN)_x$
2078.2	2009.3	1.0343	+	$V(NN)_x$
2046.8	1977.8	1.0349	+	$V(NN)_x$
2039.0	1971.1	1.0344	+	$V(NN)_x$
2011.9	1945.2	1.0343	+	$V(NN)_x$
1969.7	1904.1[b]	1.0345	+	$V(NN)_2$
1945.0	1880.7[c]	1.0342	−	VNN
1798.0 w	1738.1	1.0345	−	minor species
1754.5 w	1696.2	1.0344	−	minor species
1709.1	1657.7[d]	1.0341	−	$V(N_2)$
1641.4	1568.8[d]	1.0344	+	$(V_2)(N_2)$
1026.2	999.4	1.0268	−	VN
1020.3	993.6	1.0269	+	(NN)VN
1014.4	987.9	1.0268	+	$(NN)_xVN$
1010.6	984.2	1.0268	+	$(NN)_xVN$
1008.1	981.4	1.0272	++	site
1002.8	976.5	1.0269	++	$(NN)_xVN$
997.8	971.4	1.0272	++	$(NN)_xVN$
563	552[e]	1.020	+	$V(NN)_4$
510.0	497.5[f]	1.0243	+	$V(NN)_x$
487.2	476.5[f]	1.0225	−	$V(NN)_x$
480.7	469.3	1.0243	−	site

[a] Annealing behavior: +, increase; −, decrease. [b] Triplet with 1945 cm^{-1} intermediate component using mechanical mixture and sextet using statistical mixture. [c] Doublet using mechanical mixture and quartet with 1914, 1912 cm^{-1} intermediate components using statistical mixture. [d] Doublets using mechanical mixture and triplets with 1681.5 and 1613 cm^{-1} intermediate components using statistical mixture. [e] Pentet as in pure $^{14}N_2$ + $^{15}N_2$, [f]Intermediate components at 504.8 and 482.1 cm^{-1} using $^{14}N_2$ + $^{15}N_2$.

V + N_2. Laser-ablated V atoms condensed with pure nitrogen gave product bands in each region that are listed in Table 2; the N_3 radical[26] was observed at 1657.5 cm^{-1}, which confirms the formation of N atoms in these experiments. Spectra in the upper region were dominated by bands at 2098.7 and 2046.3 cm^{-1} which gave way on annealing to a very strong sharp 2137.7 cm^{-1} band, as is shown in Figure 1. Spectra in the middle region revealed a 997.0 cm^{-1} band which increased on annealing. Spectra in the lower region were dominated by 562.8 and 486.1 cm^{-1} bands, which decreased on annealing while a 455.6 cm^{-1} band increased markedly. Again similar spectra were observed for $^{15}N_2$, and product absorptions are given in Table 2.

One experiment was done with a $^{14}N_2$ + $^{15}N_2$ mixture and spectra are shown at the top of Figure 2 for deposition and annealing to 30 K; note growth of the 997.0 and 970.6 cm^{-1} bands and satellites. Further annealing to 35 K slightly increased but annealing to 40 K slightly decreased these bands.

Cr + Ar/N_2. Laser-ablated Cr atoms were codeposited with 2% N_2 in argon, and a weak band is observed at 1044.3 cm^{-1} with weaker bands at 1042.7 and 1030.0 cm^{-1}. A weak sharp CrO_2 band is observed at 965.4 cm^{-1},[24] along with weak NNCrO absorption at 857.0 and CrO at 846.3 cm^{-1}.[24] Annealing to 30

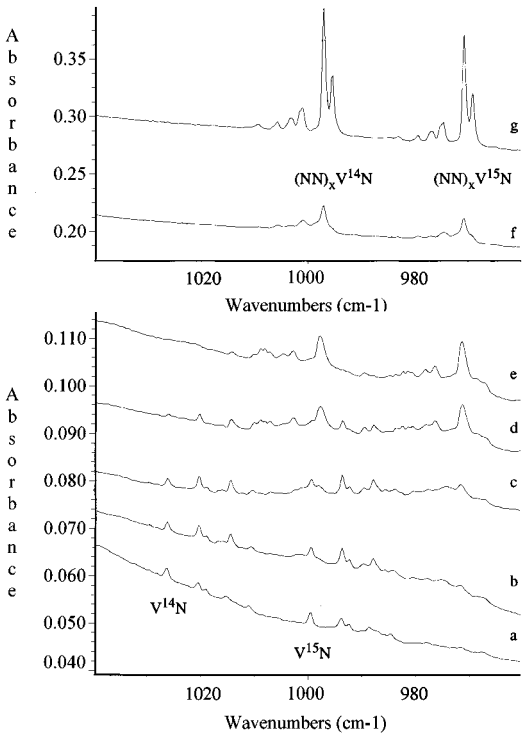

Figure 2. Infrared spectra in the 1040−960 cm^{-1} region for laser-ablated V atoms codeposited with nitrogen. (a) 2% $^{14}N_2$ + 2% $^{15}N_2$ in argon codeposited at 6−7 K for 1 h, (b) after annealing to 25 K, (c) after annealing to 30 K, (d) after annealing to 40 K, (e) after annealing to 43 K, (f) pure $^{14}N_2$ + $^{15}N_2$ codeposited at 10−11 K for 1 h, and (g) after annealing to 30 K.

K increased the 1044.3 cm^{-1} band, the 1042.6 cm^{-1} satellite, and the 1030.8 cm^{-1} absorption and decreased the 965.4 cm^{-1} isolated CrO_2 band in favor of a 973.7 cm^{-1} band due to NN−CrO_2.[24] Further annealing to 40 K decreased these bands and increased absorption at 1030.8 and 1014.2 cm^{-1}. A similar experiment using $^{15}N_2$ in argon gave weak bands shifted to 1017.0 and 1015.3 cm^{-1} instead of the 1044.3 and 1042.7 cm^{-1} features, and the broad bands remaining on annealing shifted to 1004.6 and 987.0 cm^{-1}.

The upper region contained a complicated structure beginning at 2215 cm^{-1} and containing broad features at 2151, 2139, and 2083 cm^{-1}; annealing decreased the upper band and increased the lower features. A weak sharp 1968.9 cm^{-1} band increased on annealing to 35 K and then decreased, and a broad 1613.7 cm^{-1} band appeared. A band appeared at 548.3 cm^{-1} on annealing. The band profile was shifted with $^{15}N_2$ beginning at 2140 cm^{-1} and including 2080, 2069, 2010, and 1904.4 cm^{-1} peaks. Annealing decreased the 2140 cm^{-1} band, increased the others, and produced a weak 536.3 cm^{-1} band.

Figure 3 shows spectra for the reaction of Cr atoms with a statistical isotopic mixture in argon prepared by discharge during deposition at 6−7 K; the same bands were observed first without discharge. Notice the sets of weak bands beginning at 1044.3 and at 1017.0 cm^{-1} in the deposited sample (Figure 3a); a very weak CrO_2 band at 965.4 cm^{-1} and weak bands at 879.7, 857.0, and 846.3 cm^{-1} due to CrO and NN complexes are not shown.[24] Annealing to 30 K increased these bands slightly (Figure 3b), but annealing to 39 K decreased the first member and increased the second member of each set and produced new bands at 1031.8 and 1014.2 cm^{-1} in the upper isotopic set and at 1004.6 and 987.0 cm^{-1} in the lower isotopic set (Figure 3c). Further annealing to 43 K favored the 1031.8 and 1004.6 cm^{-1} bands (Figure 3d), but annealing to 46 K increased the bands at 1014.2 and 987.0 cm^{-1} (Figure 3e), which are the only survivors of a fast anneal to 48 K (Figure 3f). The 1968.9−1904.4 cm^{-1} band system gave a 1930.1 cm^{-1} intermediate component with $^{14}N_2$ + $^{15}N_2$, and the discharged statistical mixture gave three more bands each with subsplittings (1952.4, 1950.5 cm^{-1}; 1937.2, 1936.9, 1935.4 cm^{-1}; 1920.4, 1918.5 cm^{-1}). A 1613.7, 1588.4, 1560.1 cm^{-1} triplet appeared on annealing.

TABLE 2: Infrared Absorptions (cm^{-1}) from Codeposition of Laser-Ablated Vanadium Atoms with Excess Nitrogen at 10 ± 1 K

$^{14}N_2$	$^{15}N_2$	*R*(14/15)	anneal[a]	assign
2327.6	2249.8	1.0346	−	N_2
2237.0	2162.4	1.0345	+	$(NN)_xVN$
2216 w	2144	1.0336	−	?
2174 w	2102 w	1.0343	+	?
2137.7	2066.9[b]	1.0343	++	$V(NN)_6$
2132.4	2061.5	1.0344	+	$V(NN)_6$ site
2098.7	2028.9[b]	1.0344	−	$V(NN)_x$
2075.4	2006.6[b]	1.0343	+	$V(NN)_x$
2046.3	1978.0[b]	1.0345	−	$V(NN)_4$
2003.4	1937.6	1.0339	−	N_3^-
1970.0	1904.8[b]	1.0342	−	?
1874.7	1812.5	1.0343	+	$(NN)_xV(N_2)$
1861.9	1800.4	1.0342	+	$(NN)_xV(N_2)$
1851.6	1790.2	1.0343	−	$(NN)_xV(N_2)$
1657.5	1603.4	1.0337	−	N_3
1009.5	982.9	1.0271	−	$(NN)_xVN$
1001.1	974.6	1.0272	+,−	$(NN)_xVN$
997.0	970.0	1.0272	+	$(NN)_xVN$
995.5	969.1	1.0272	+	site
928.9	904.4[c]	1.0271	+	(VNVN)
872.4	871.1	1.0015	+	(NVO)
820.1	799.9[e]	1.0253	+	NVN
774.6	754.6[e]	1.0265	−	?
746.2	726.2[e]	1.0275	+	$(VN)_2$
672.7	655.2	1.0267	+,−	?
562.8	551.7[f]	1.0201	−	$V(NN)_4$
486.1	475.4[g]	1.0225	+	$V(NN)_x$
470.6	458.8[g]	1.0257	−	$V(NN)_x$
455.6	445.0[g]	1.0238	++	$V(NN)_6$

[a] Annealing behavior: +, increase, −, decrease. [b] Intermediate absorptions for the highest four bands in $^{14}N_2$ + $^{15}N_2$ experiments were weak and could not be definitely identified; the 1970.0−1904.8 cm^{-1} band had no intermediate component. [c] Quartet using $^{14}N_2$ + $^{15}N_2$ with intermediate components at 925.6 and 906.5 cm^{-1}. [d] Oxygen-18 shift to 837.3 cm^{-1}, doublet with oxygen isotopic mixtures. [e] Triplets using $^{14}N_2$ + $^{15}N_2$ with intermediate components at 810.3, 762, and 736.5 cm^{-1}, respectively. [f] Resolved 1/4/6/4/1 pentet at 562.5, 560.0, 537.5, 554.9, 551.9 cm^{-1} in $^{14}N_2$ + $^{15}N_2$ sample. [g] Resolved 1/2/1 triplets with central component at 489.9, 465.1, 450.6 cm^{-1}, respectively, using $^{14}N_2$ + $^{15}N_2$.

Cr + N_2. Chromium atoms codeposited with pure nitrogen gave a very strong, sharp band at 2112.6 cm^{-1} and a strong band at 548.5 cm^{-1}, as shown in Figure 4a. A weaker (A = 0.05) 1795.1 cm^{-1} band was also observed. Annealing had little effect on the former bands, but the latter decreased in favor of a sharp 1803.5 cm^{-1} band. Weak bands were observed for N_3^- and N_3 radical as reported previously.[26] The spectrum from 1050 to 750 cm^{-1} reveals new nitride product bands listed in Table 3. Sharp new bands at 1044.2 and 875.7 cm^{-1} shift to 1016.9 and 854.2 cm^{-1} with $^{15}N_2$.

Figure 5 shows this region of the spectrum for the $^{15}N_2$ sample; note the absence of CrO_2 absorptions in the 980−970 cm^{-1} region. Photolysis had little effect on the sample. Thermal cycles stepwise to 25, 30, and 35 K caused pronounced changes in the spectra as shown in Figure 5. Sharp new bands appear at 1000.2, 988.8, 949.6, 930.0, and 861.7 cm^{-1} as the 854.2 cm^{-1} band increases markedly, whereas the 1016.9 cm^{-1} band decreases slightly. Chromium isotopic splittings are observed on the strong 854.2 cm^{-1} band at 852.0 and 849.9 cm^{-1}, on the 861.7 cm^{-1} band at 859.5 and 857.4 cm^{-1}, and

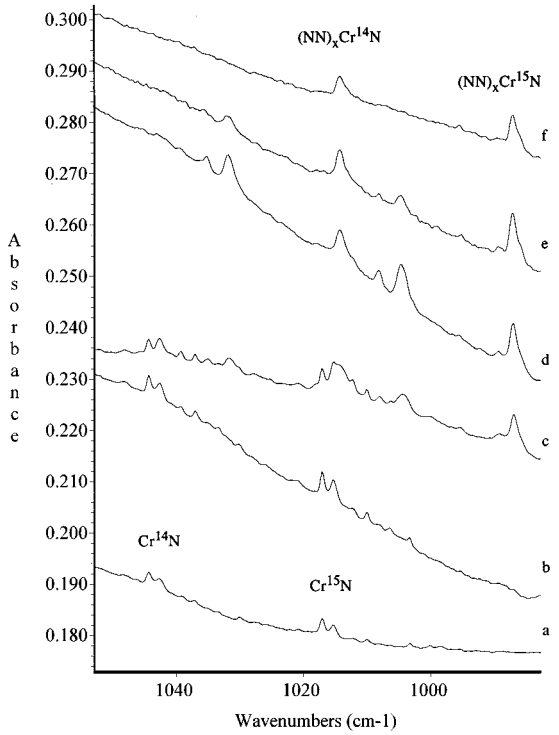

Figure 3. Infrared spectra in the 1060−980 cm^{-1} region for laser-ablated Cr atoms codeposited with isotopic nitrogen mixture in argon at 6−7 K for 1.5 h. (a) 2% $^{14}N_2$ + 2% $^{15}N_2$ in argon discharged to give 1% $^{14}N_2$ + 2% $^{14}N^{15}N$ + 1% $^{15}N_2$ in argon during codeposition, (b) after annealing to 30 K, (c) after annealing to 39 K, (d) after annealing to 43 K, (e) after annealing to 46 K, and (f) after annealing to 48 K.

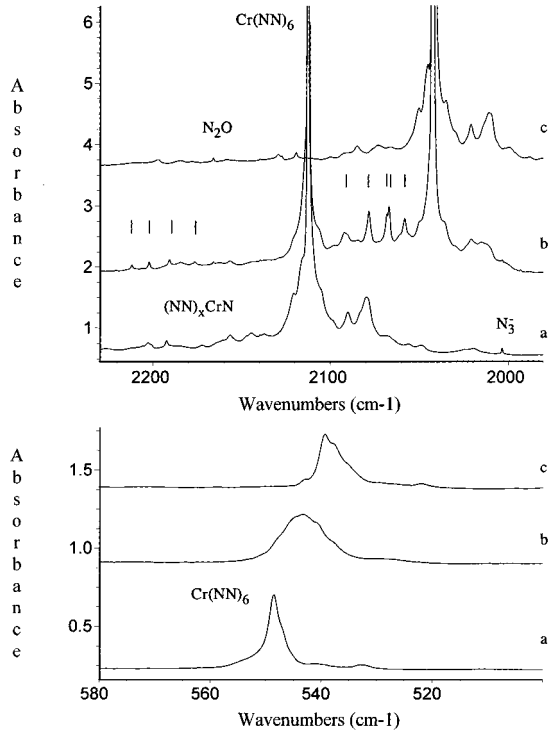

Figure 4. Infrared spectra in the 2230−1980 and 580−500 cm^{-1} regions for laser-ablated Cr atoms codeposited with isotopic nitrogen samples at 10 ± 1 K for 1 h. (a) pure $^{14}N_2$, (b) 50% $^{14}N_2$ + 50% $^{15}N_2$, and (c) pure $^{15}N_2$. The vertical slashes indicate symmetric and antisymmetric modes, respectively, of $Cr(NN)_6$ isotopic molecules of lower symmetry.

on the 988.8 cm^{-1} band at 986.6 cm^{-1}. In the upper region, the very strong, sharp band shifts to 2042.0 and the lower band to 539.4 cm^{-1} as shown in Figure 4c.

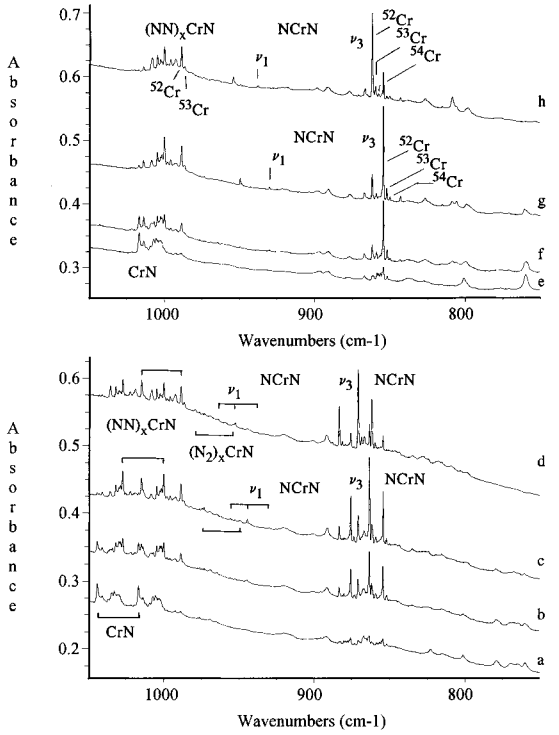

Figure 5. Infrared spectra in the 1050−750 cm^{-1} region for laser-ablated Cr atoms codeposited with isotopic nitrogen samples at 10 ± 1 K for 1 h. (a) 50% $^{14}N_2$ + 50% $^{15}N_2$, (b) after annealing to 25 K, (c) after annealing to 30 K, (d) after annealing to 35 K, (e) pure $^{15}N_2$, (f) after annealing to 25 K, (g) after annealing to 30 K, and (h) after annealing to 35 K.

Both mechanical ($^{14}N_2$ + $^{15}N_2$) and statistical ($^{14}N_2$ + $^{14}N^{15}N$ + $^{15}N_2$) isotopic mixtures were studied. The spectrum in the upper region (Figure 4b) shows two very strong 2112.6 and 2042.0 cm^{-1} bands plus four weak, sharp intermediate bands given in Table 1 for the mechanical mixture, and the lower region gives a single 544.9 cm^{-1} band. The statistical mixture gave a strong 2112.6, 2077.7, 2142.0 cm^{-1} triplet and a single broader 543 cm^{-1} band. The 1795.1 and 1803.5 cm^{-1} bands became doublets with the mechanical mixture and 1/2/1 triplets with the statistical mixture, adding intermediate bands at 1774.0 and 1765.7 cm^{-1}.

Of most interest are the mixed isotopic spectra shown in Figure 5 for the mechanical mixture (the statistical mixture gave the same splittings). The first $^{14}N_2$ product absorption at 1044.2 cm^{-1} gave a doublet with a $^{15}N_2$ counterpart at 1016.9 cm^{-1}, simply the sum of pure isotopic spectra. The same doublet structure was observed for all product bands down to 1015.1 and 988.8 cm^{-1}. However, the strong annealing band at 875.7 cm^{-1} gave a 1/2/1 triplet with an intermediate component at 863.2 cm^{-1}, and the strong 883.3 cm^{-1} band favored on higher temperature annealing also gave a 1/2/1 triplet with intermediate at 870.7 cm^{-1}. The weaker 956.1 and 963.8 cm^{-1} bands, which track with the 875.7 and 883.3 cm^{-1} bands on annealing, respectively, also gave triplets.

Mn + Ar/N_2. Laser-ablated Mn atoms codeposited with 2% N_2 in argon gave weak new bands at 1054.9 and 1047.0 cm^{-1}, a stronger band at 916.1 cm^{-1}, a weak MnO band at 833.1 cm^{-1}, and a sharp NNMnO band at 868.3 cm^{-1}.[25] Annealing to 30 K increased the 1054.9 and 1047.0 cm^{-1} bands and decreased the 916.1 cm^{-1} band. A similar experiment with $^{15}N_2$ shifted the weak bands to 1027.1 and 1019.4 cm^{-1} and the sharp new band to 891.9 cm^{-1}. The upper complex region contained new bands at 2106.4, 2055.0, 2036.2, and 2020.2 cm^{-1}; the sharp 2036.2 cm^{-1} band decreased on annealing, and the others

TABLE 3: Product Absorptions (cm^{-1}) Produced by Codepositing Laser-Ablated Cr Atoms with Excess Nitrogen at 10 ± 1 K

$^{14}N_2$	$^{15}N_2$	$^{14}N_2 + {}^{15}N_2$	R(14/15)	anneal[a]	assign
2192.4	2119.4		1.0344	+	$(NN)_xCrN$
2156.3	2085.0		1.0342	+,−	$(NN)_xCrN$
2112.6	2042.0	2112.6, 2092.2, 2078.4, 2067.0, 2058.3, 2042.0	1.0346	0	$Cr(NN)_6$
2080.3	2011.2		1.0344	+,−	$Cr(NN)_x$
1803.5	1743.9	1003.5, 1743.9	1.0342	+	$(NN)_xCr(N_2)$
1795.1	1735.8	1795.1, 1735.8	1.0342	−	$(NN)_xCr(N_2)$
1657.5	1603.4	quartet	1.0337	−	N_3
1044.2	1016.9	doublet	1.0269	−	CrN
1041.0	1013.9	doublet	1.0267	−	$(NN)_xCrN$
1035.7	1008.6	doublet	1.0269	+,−	$(NN)_xCrN$
1027.4	1000.2	doublet	1.0272	+,−	$(NN)_xCrN$
1019.4	992.6	doublet	1.0270	+	$(NN)_xCrN$
1015.1	988.8	doublet	1.0266	+	$(NN)_x{}^{52}CrN$
1013.0	986.6		1.0267	+	$(NN)_x{}^{53}CrN$
980.1	954.3		1.0270	+	$(N_2)_xCrN$?
975.3	949.6		1.0271	+,−	$(N_2)_xCrN$?
963.8	937.8	963.8, 952.7, 937.8	1.0277	+	NCrN(ν_1) site b
956.1	930.0	955.9, 944.7, 930.0	1.0281	+,−	NCrN(ν_1) site a
883.3	861.7	883.3, 870.7, 861.7	1.0251	+	$N^{52}CrN$(ν_3) site b
881.2	859.5	881.2, 868.6, 859.5	1.0253	+	$N^{53}CrN$(ν_3) site b
879.2	857.4	879.2, 857.4	1.0254	+	$N^{54}CrN$(ν_3) site b
875.7	854.2	875.7, 863.2, 854.2	1.0252	+,−	$N^{52}CrN$(ν_3) site a
873.5	852.0	873.5 852.0	1.0252	+,−	$N^{53}CrN$(ν_3) site a
871.4	849.9		1.0253	+,−	$N^{54}CrN$(ν_3) site a
847.1	826.6		1.0246	+,−	$(NN)_xCrN_2$
829.6	808.8	834.3, 828.1, 817.7, 809.1	1.0257	+	$(NN)_xCrN_2$
822.7	801.1	822.7, 815.2, 801.1	1.0270	−	$(CrN)_2$?
778.8	759.7	778.8, 769.5, 764.4, 759.7	1.0251	−	(CrNCrN) ?
690.8	673.8	690.8, 683.0, 673.8	1.0252	+	$(N_2)CrN_2$ site b
685.9	669.1	685.9, 678.2, 669.1	1.0251	+,−	$(N_2)CrN_2$ site a
548.5	539.4	544.9 broad	1.0169	0	$Cr(NN)_6$

[a] Annealing behavior: increase, +; no change, (0) decrease, −.

TABLE 4: Infrared Absorptions (cm^{-1}) from the Codeposition of Laser-Ablated Manganese Atoms with 2% N_2 in Argon at 10 K

$^{14}N_2$	$^{15}N_2$	R(14/15)	anneal[a]	assign
2106.4	2036.3	1.0344	+	$Mn(NN)_5$
2055.0	1988.2	1.0336	++	$Mn(NN)_x$
2036.2	1968.1	1.0346	+,−	$Mn(NN)_x$
2020.2	1953.0	1.0344	+,−	$Mn(NN)_x$
1865.8	1803.8	1.0344	−	?
1850.1	1789.0[b]	1.0342	+	$(NN)_xMn(N_2)$
1819.3	1759.1[b]	1.0342	−	$Mn(N_2)$
1786.6	1727.4	1.0343	−	?
1054.9	1027.1	1.0271	+	$(NN)_xMnN$
1050.5	1022.9	1.0270	−	$(NN)_xMnN$
1047.0	1019.4	1.0271	+,−	$(NN)_xMnN$
916.1	892.0	1.02702	−	MnN
868.3	868.3		−	NNMnO
833.1	833.1		−	MnO
813.3	813.3		−	MnOMn
808.3	808.3		−	MnOMn
787.9 w	766.8	1.0275	−	?
696.2 w	678.1	1.0267	+	?
654.2 w	637.2	1.0267	+	?

[a] Annealing behavior: +, increase; −, decrease. [b] Intermediate components in statistical mixture at 1819.1 and 1789.4 cm^{-1}.

increased. These bands shifted to 2036.3, 1990, 1967.2, and 1953.0 cm^{-1} with the $^{15}N_2$ reagent as listed in Table 4.

The spectrum of Mn codeposited with a discharged mixture of 2% $^{14}N_2$ + 2% $^{15}N_2$ in argon is shown in Figure 6; the same bands were observed first without discharge. Two sets of weak bands were observed beginning at 1054.9 and 1027.1 cm^{-1}, and two stronger bands were observed at 916.1 and 891.9 cm^{-1}, along with NNMnO (868.3 cm^{-1}), MnO (833.1 cm^{-1}), and Mn_2O (813.3 cm^{-1}) (Figure 6a); note the absence of OMnO at 948.0 cm^{-1}.[25] Annealing to 30 and 35 K slightly increased the 1054.9 and 1027.1 cm^{-1} band systems, decreased the 916.1 and 891.9 cm^{-1} bands, and decreased the MnO band (Figure 6b,c).

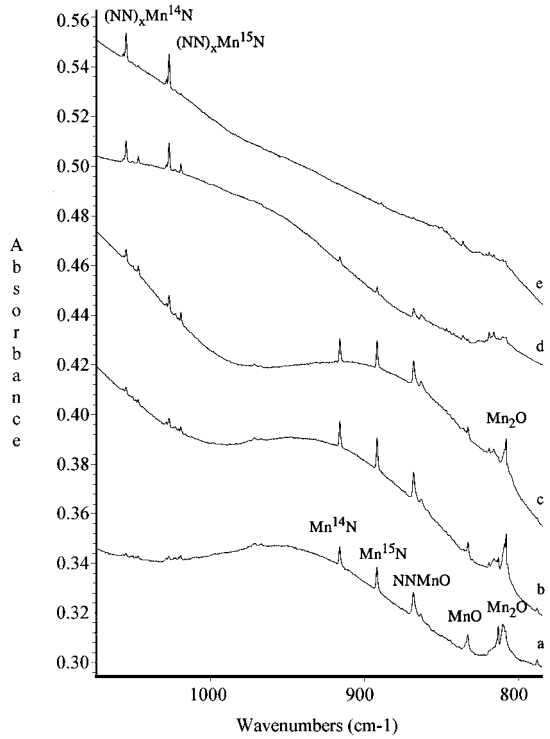

Figure 6. Infrared spectra in the 1060−790 cm^{-1} region for laser-ablated Mn atoms codeposited with isotopic mixture in argon at 6−7 K for 1.5 h. (a) 2% $^{14}N_2$ + 2% $^{15}N_2$ in argon discharged to give 1% $^{14}N_2$ + 2% $^{14}N^{15}N$ + 1% $^{15}N_2$ in argon during codeposition, (b) after annealing to 30 K, (c) after annealing to 35 K, (d) after annealing to 40 K, and (e) after annealing to 43 K.

Further annealing to 40 K markedly increased the former and decreased the latter bands (Figure 6d), and annealing to 43 K increased the 1054.9 and 1027.1 cm^{-1} bands still more and

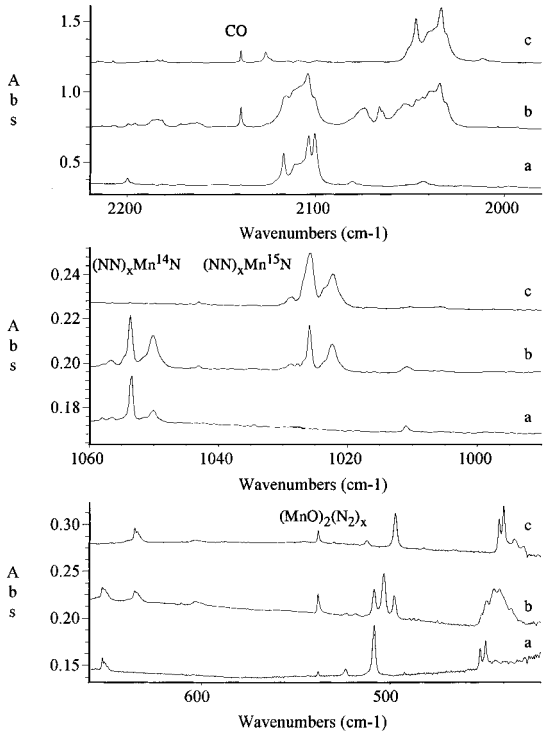

Figure 7. Infrared spectra in the 2200−1980, 1060−980, and 660−420 cm^{-1} regions for laser-ablated Mn atoms codeposited with isotopic nitrogen samples at 10 ± 1 K for 1 h. (a) pure $^{14}N_2$, (b) 50% $^{14}N_2$ + 50% $^{15}N_2$, and (c) pure $^{15}N_2$.

destroyed the 916.1 and 891.9 cm^{-1} bands (Figure 6e). A final rapid temperature cycle to 46 K decreased the 1054.9 and 1027.1 cm^{-1} bands and increased the noise level (not shown); the latter bands approach the major absorptions in the nitride region using pure nitrogen.

Mn + N_2. The spectrum of Mn in pure nitrogen is more complicated than that found for Cr in the complex region but less involved than that in the nitride region. Figure 7 shows the upper and lower complex regions: very strong sharp bands were observed at 2116.9, 2103.5, and 2100.4 cm^{-1} with weaker bands at 2199.7 and 2080.1 cm^{-1}, and new bands appeared at 523.7, 508.5, 452.5, and 449.6 cm^{-1}. Not shown is a weaker 1844.2 cm^{-1} band. Three distinctly different annealing behaviors were observed: the 2199.7, 2116.9, 2080.1, and 523.7 cm^{-1} bands increased about 50%, the 2110 cm^{-1} shoulder and 508.5 cm^{-1} absorption decreased about 50%, and the close doublets increased about 10%. Figure 7 also shows the nitride region: a single sharp 1053.7 cm^{-1} band with 1050.1 cm^{-1} satellite is observed, which increases slightly on annealing, along with weak MnO_2 and MnO bands at 969.5 and 843.6 cm^{-1} and sharp, weak new 858.9 and 842.0 cm^{-1} bands, which increased 3-fold on annealing.

All of these bands are shifted in the $^{15}N_2$ matrix reaction. The positions are given in Table 5, and the isotopic spectra are compared in Figure 7. When a mechanical mixture of $^{14}N_2$ and $^{15}N_2$ was employed, only the pure isotopic bands, unshifted ±0.1 cm^{-1}, were observed in the 1053.7−1025.9 cm^{-1} region, but a triplet was observed at 858.7, 846.9, 838.4 cm^{-1}. New bands were found in the complex region, in addition to the pure isotopic bands at 2172.0, 2073.1, 2064.3, 518.5, 503.5, and 445.7 cm^{-1}. Other such bands in the upper region may be masked by the major absorptions.

Calculations. Density functional theory using the Gaussian 94 code,[27] 6-311 + G* basis sets, and BPL functional was employed to calculate structures and frequencies for the simplest product molecules expected here. V, Cr, and Mn mononitrides are calculated at the BPL level to be lower than the dissociation limits M + N by 138, 105, and 83 kcal/mol, respectively. Results for VN and CrN may be compared with those from MCSCF, MRCI, and LDF calculations;[11,28] results for MnN in the lowest triplet and quintet states are also listed in Table 6. The bent NN−VN complex was also computed and the V−N fundamental found to red-shift by 22 cm^{-1} on complexation by N_2 with a 16.3 kcal/mol binding energy. The bent NN−CrN molecule failed to converge. The bent NN−MnN complex was calculated to have a stable triplet state bound by 15.6 kcal/mol with a strong Mn−N stretching frequency at 1030 cm^{-1} and a stable quintet state bound by 6.6 kcal/mol with a strong Mn−N stretching mode at 952 cm^{-1}.

TABLE 5: Product Absorptions (cm^{-1}) Produced by Codepositing Laser-Ablated Mn Atoms with Excess Nitrogen at 10 K

$^{14}N_2$	$^{15}N_2$	*R*(14/15)	anneal[a]	assign
2199.7	2126.5	1.0344	+	$Mn_2(NN)_{10}$
2142.5	2071.4	1.0343	++	?
2116.9	2046.8	1.0342	+	$Mn_2(NN)_{10}$
2103.5	2036.5	1.0329	+	$Mn(NN)_5$
2100.4	2033.4	1.0329	+	$Mn(NN)_5$
2080.1	2012.0	1.0338	+	$Mn_2(NN)_{10}$
1844.2	1783.1	1.03427	−	$(NN)_xMn(N_2)$
1657.5	1603.4	1.0337	−	N_3
1053.7	1025.9	1.02706	+,−	$(NN)_xMnN$
1050.1	1022.3	1.02719	−	$(NN)_xMnN$ site
858.7	838.5[b]	1.0241	+	NMnN
843.6	843.6		−	MnO
842.0	841.8		+	NMnO
652.7	635.7	1.0267	+,−	?
538.3	538.3		+	$(MnO)_2(N_2)_x$
523.7	512.4	1.0221	+,−	$Mn_2(NN)_{10}$
508.5	497.3	1.0225	−	$Mn(NN)_x$
452.5	442.4	1.0228	+	$Mn(NN)_5$
449.6	439.9	1.0221	+	$Mn(NN)_5$

[a] Annealing behavior: +, increase; −, decrease. [b] Intermediate component at 846.9 cm^{-1} using $^{14}N_2$ + $^{15}N_2$.

We should point out that although bent NCrN and NMnN energies are higher than M + N_2 energies, they are significantly lower than M + 2N dissociation limits by 181 and 166 kcal/mol, respectively. Our experiments show, as will be discussed in the next section, that the formation of NCrN is due to the reaction of N and CrN and not Cr and N_2. An energy barrier between NCrN and CrNN can justify the formation and stability of bent dinitrides. For all three metals, the strongest absorptions are predicted in the 1900 cm^{-1} region for MNN molecules, the cyclic M(N_2) molecules 100−800 cm^{-1} lower, and the bent NMN molecules even below the MN molecules, in the 1000−700 cm^{-1} region. These approximate calculations are only intended to serve as a guide for the experimental identification of new molecules.

Calculations were done for three isomers of VN_2, CrN_2, and MnN_2, and the results are summarized in Table 7. The linear VNN isomer was the most stable followed by cyclic V(N_2) in $^6A_1$, $^4B_2$, and $^2A_1$ states and finally $^2B_2$ bent NVN. The bent molecule is lower by 0.6 and 236 kcal/mol than V + N_2 and V + 2N, respectively. For Cr and Mn, the calculations do not present the same picture; all isomers are above the M + N_2 dissociation limit. For example, the lowest CrNN ($^5A'$) and MnNN ($^4A''$) states are 14 and 12 kcal/mol higher, respectively, and NCrN and NMnN are 55 and 69 kcal/mol higher, respectively, than the metal atoms + N_2. Note that the same relationship was calculated recently for MoN_2 and WN_2 molecules.[29] Clearly, the present DFT calculations must be considered only as a first approximation, and higher levels of theory are required for a better description of these systems.

TABLE 6: Density Functional Calculations of Harmonic Frequencies, Infrared Intensities, and Bond Lengths for VN, CrN, and MnN and Dinitrogen Complexes Using 6-311 + G* Basis Sets

		VN (Triplet)[a]	
BPL	1073 cm^{-1}, 117 km/mol, 1.565 Å	MCSCF[b]	1025 cm^{-1}, 1.607 Å
B3LYP	1061 cm^{-1}, 1.561 Å	expt[c]	1033 cm^{-1}, 1.574 Å
		CrN ($^4\Sigma$)[a]	
BPL	1017 cm^{-1}, 105 km/mol, 1.555 Å	MCSCF[b]	854 cm^{-1}, 1.619 Å
B3LYP	846 cm^{-1}, 1.535 Å		
		MnN (Triplet)[a,d]	
BPL	1022 cm^{-1}, 50 km/mol, 1.529 Å		
B3LYP	820 cm^{-1}, 1.522 Å		
		MnN (Quintet)[a,d]	
BPL	890 cm^{-1}, 91 km/mol, 1.597 Å		
B3LYP	706 cm^{-1}, 1.636 Å		
		NN−VN (Triplet)	
BPL	1051 cm^{-1}, 108 km/mol, 1.574 Å, 2072 cm^{-1}, 949 km/mol, 1.129 Å	NN−V−N = 104°,	NN−VN = 2.040 Å
		NN−MnN (Triplet)[e,f]	
BPL	1030 cm^{-1}, 119 km/mol, 1.548 Å, 2076 cm^{-1}, 596 km/mol, 1.132 Å	NN−Mn−N = 111°,	NN−MnN = 1.898 Å
		NN−MnN (Quintet)[e,g]	
BPL	952 cm^{-1}, 141 km/mol, 1.587 Å, 2085 cm^{-1}, 770 km/mol, 1.126 Å	NN−Mn−N = 130°,	NN−MnN = 2.041 Å
		NN (Singlet)	
BPL	2327 cm^{-1}, 0 km/mol, 1.107 Å		

[a] Lowest energy state calculated for this multiplicity. [b] Reference 11. [c] Reference 7. [d] Quintet more stable by 0.8 kcal/mol with both functionals. [e] Triplet is more stable by 8.2 kcal/mol. [f] Triplet NN−MnN complex bound by 15.6 kcal/mol. [g] Qunitet NN−MnN complex bound by 6.6 kcal/mol.

TABLE 7: Density Functional Calculations of Frequencies and Structures for VN_2, CrN_2, and MnN_2 Isomers

	E(kcal/mol)	structure	ν_1(I)[a]	ν_2(I)	ν_3(I)
VNN (sextet)	0	1.141, 1.968 Å linear	1980 (882)	391 (24)	250 (2)
V(N_2) cycle ($^6A_1$)	+12	1.155, 2.200 Å	1907 (530)	289 (10)	225 (9)
($^4B_2$)	+16	α = 30° 1.204, 1.982 Å α = 35°	1650 (276)	414 (8)	423 (3)
($^2A_1$)	+24	1.339, 1.751 Å α = 45°	1169 (106)	663 (29)	402 (0)
NVN ($^2B_2$)	+26	1.630 Å α = 102°	986 (21)	338 (6)	744 (50)
CrNN ($^5A'$)	0	1.162, 1.951 Å α = 178°	structure not converged due to oscillation		
($^3A''$)	21	1.151, 1.831 Å	1923 (442)	481 (19)	295 (3)
Cr(N_2) ($^5B_2$)	1	1.197, 1.984 Å α = 35°	1690 (285)	448 (0)	412 (15)
($^3B_1$)	29	1.273, 1.835 Å α = 40°	1435 (234)	466 (14)	387 (11)
($^1A_1$)	43	1.232, 1.835 Å α = 39°	1502 (149)	561 (45)	429 (1)
NCrN ($^3B_2$)	41	1.610 Å α = 101°	994 (72)[b]	362 (0)	721 (48)
MnNN ($^4A''$)	0	1.154, 1.774 Å α = 177°	1869 (2380)	481 (164)	288 (20)
($^2A''$)	+17	1.151, 1.764 Å α = 180°	1976 (646)	537 (16)	237 (0)
($^6B_2$)	−3	1.156, 2.206 Å α = 31°	1933 (208)	238 (6)	175 (2)
($^4B_2$)	+5	1.172, 2.017 Å α = 34°	1830 (284)	374 (8)	373 (19)
Mn(N_2) ($^2B_1$)	+26	1.210, 1.878 Å α = 38°	1601 (231)	464 (8)	415 (23)
NMnN ($^4A_2$)	+58	1.607 Å α = 108°	965 (33)	312 (1)	625 (71)

[a] Frequencies, cm^{-1} (intensities, km/mol). [b] For $^{14}N^{52}Cr^{14}N$ isotopic molecule; frequencies 981, 357, 711 cm^{-1} for $^{14}N^{52}Cr^{15}N$; 967, 352, 702 cm^{-1} for $^{15}N^{52}Cr^{15}N$ molecule.

Discussion

The new vanadium, chromium, and manganese nitride molecules and dinitrogen complexes will be identified.

VN. The sharp weak new band at 1026.2 cm^{-1} in solid argon decreases on stepwise annealing while sharp bands increase at 1020.3, 1014.4, and ultimately 997.8 cm^{-1}. These bands exhibit

sharp nitrogen-15 counterparts at 999.4, 993.6, 987.9, and 971.4 cm^{-1}, which define nitrogen 14/15 frequency ratios 1.0268, 1.0269, 1.0268, and 1.0272, respectively. These values are in excellent agreement with the harmonic VN diatomic ratio (1.0272) and attest to the pure V−N stretching character of these absorptions. Normal cubic anharmonicity accounts for the observed ratios being slightly lower than the harmonic ratios. These bands showed no intermediate components with discharged (statistical) mixed isotopic nitrogen, so a single nitrogen atom is involved in these vibrations. In solid nitrogen a sharp isotopic doublet at 997.0 and 970.6 cm^{-1} also increased on annealing and revealed the diatomic ratio (1.0272) and was only 0.8 cm^{-1} lower than the dominant nitrogen isotopic doublet surviving past 40 K annealing in solid argon.

The sharp 1026.2 band is here assigned to VN isolated in solid argon. This band is in reasonable agreement with the gas-phase fundamental reported at approximately 1020 ± 5 cm^{-1}.[7] Three possibilities for reconciliation between the gas phase and argon matrix must be considered: (1) if TiN is an appropriate guide, then the 1032.4 cm^{-1} argon matrix[30] and 1039.5 cm^{-1} gas-phase[6] fundamentals suggest a 7 cm^{-1} *red-shift* by the matrix, and accordingly, the gas-phase VN fundamental may actually be 1033 ± 5 cm^{-1}, (2) VN is blue-shifted by the argon matrix some 6 cm^{-1}, or (3) the stronger 1020.3 cm^{-1} band is also due to VN in a different matrix site, which is in agreement with the gas-phase fundamental. Observations[23,31] with TiO and VO suggest that the first option is most likely.

The increase of the 1020.3 cm^{-1} band on annealing to 35 K suggests complexation by N_2 and assignment of the new bands at 1020.3, 1014.4, 1010.6 (or 1008.1), 1002.8, and 997.8 cm^{-1} in solid argon and the almost identical band at 997.0 cm^{-1} in solid nitrogen to the $(NN)_xVN$ complexes. The evolution of bands in Figure 2 from 1026.2 to 997.8 cm^{-1} on annealing in solid argon and the 997.0 cm^{-1} band in solid nitrogen provides a convincing picture for the sequential attachment of dinitrogen ligands to the VN center.

The lowest VN triplet state harmonic vibrational fundamental was calculated at 1073 cm^{-1} by BPL/DFT, which is slightly higher than the MCSCF calculated[11] and experimental[7] values. However, the triplet NN−VN species is calculated to be bound by 16.3 kcal/mol and to exhibit a strong V−N stretching mode at 1051 cm^{-1}, red-shifted 22 cm^{-1} from the VN value, which is on the order of that found in the present matrix experiments. The N−N fundamental is predicted at 2072 cm^{-1}, red-shifted by 256 cm^{-1} from isolated N_2, and bands appear in this region for complexed dinitrogen. The 2237 cm^{-1} band is most likely due to the extensively ligated species $(NN)_xVN$.

CrN. The codeposition of laser-ablated Cr atoms with pure nitrogen forms a sharp band at 1044.2 which gives way on stepwise annealing to lower bands at 1041.0, 1035.7, 1027.4, 1019.4, and 1015.1 cm^{-1}. These bands exhibit nitrogen isotopic 14/15 ratios from 1.0266 to 1.0272, as compared to the harmonic diatomic CrN ratio of 1.0273, and isotopic splittings which are in accord with the vibration of a single N atom. Furthermore, several of these bands reveal weak satellites displaced 2.1 cm^{-1} (for ^{14}N) and 2.2 cm^{-1} (for ^{15}N) to the red which are appropriate for the ^{53}Cr in natural abundance (52/53 ratios are 1.002 07 observed, 1.002 05 harmonic calculated for ^{14}N), indicating that a single Cr atom is involved in the vibration. Hence, the above evidence strongly supports assignment of the 1044.2 cm^{-1} band to CrN and the 1041.0, 1035.7, 1027.4, and 1015.1 cm^{-1} bands to dinitrogen complexes $(NN)_xCrN$. Unfortunately, we cannot determine the maximum number of dinitrogen ligands. Finally, weak sharp bands appear at 975.3 and 980.1 cm^{-1} on annealing. These bands show the diatomic 14/15 ratio and no intermediate isotopic component so they are probably also due to CrN complexes. These bands are sharper than the strong $(NN)_xCrN$ bands, and assignment to $(N_2)_xCrN$ involving side bound N_2 ligand(s) is suggested.

The degree of interaction of uncomplexed CrN with the nitrogen matrix is revealed by the observation of a weak, sharp 1044.3 cm^{-1} band in solid argon, which exhibits a similar 1.0267 diatomic isotopic ratio. The 1044.3 cm^{-1} band is followed by a series of bands on stepwise annealing to allow diffusion and further ligation by N_2 in the sample. The spectra in Figure 3 show major bands at 1035.2 and 1031.8 cm^{-1} and the final band at 1014.2 cm^{-1} which corresponds to $(NN)_xCrN$. The 1044.3 cm^{-1} band is assigned to CrN in solid argon. There are no bands in these spectra between 800 and 1000 cm^{-1} that can be due to CrN.

Similar experiments in this laboratory[30] with Ti and N_2 in argon gave a sharp, weak 1032.4 cm^{-1} band that exhibits the diatomic 14/15 ratio and is red-shifted from the gas-phase fundamental.[6] Thus, using the same matrix shift, we predict the gas-phase fundamental of CrN at 1050 ± 10 cm^{-1}.

This fundamental frequency for CrN is some 200 cm^{-1} higher than that predicted by MCSCF and MRCI calculations.[11] It is interesting to note that simple density functional theory using the Gaussian 94 code,[27] 6-311 + G* basis sets, and BPL functional predict a quartet state with a 1017 cm^{-1} fundamental and 1.553 Å bond length for CrN. Clearly, CrN is a difficult calculational subject.

MnN. Laser-ablated Mn in pure nitrogen gives a very sharp 1053.7 cm^{-1} band with ^{15}N counterpart at 1025.7 cm^{-1} and ratio of 1.0271 compared to the harmonic diatomic value 1.0275. Annealing increases then decreases these bands *without* the family of red-shifted complex bands observed for chromium. In solid argon three weak sharp bands are observed at 1054.9, 1050.3, and 1047.1 cm^{-1} with a stronger band at 916.1 cm^{-1} (Figure 6); all show the diatomic ratio 1.0270 ± 0.0001. Note that annealing stepwise to 35 K decreases the latter band and increases the 1054.9 and 1047.1 cm^{-1} bands, then annealing to 40 K dramatically decreases the 916.1 cm^{-1} band and increases the 1054.9 and 1047.1 cm^{-1} bands, and annealing to 43 K increases the 1054.9 cm^{-1} band and essentially destroys the 1047.1 and 916.1 cm^{-1} bands. Clearly the 1054.9 cm^{-1} band is MnN complexed to the maximum number of dinitrogen molecules as is the 1053.7 cm^{-1} band in solid nitrogen. The 1047.1 cm^{-1} band is due to MnN complexed to less than the maximum number of nitrogen molecules. We are left with the possibility that MnN isolated in solid argon absorbs at 916.1 cm^{-1}. How, then, can we account for the large difference between the $(NN)_xMnN$ fundamental at 1054.9 cm^{-1} and the isolated MnN fundamental at 916.1 cm^{-1}?

The strong sharp 916.1 cm^{-1} band in solid argon that decreases on annealing in favor of the 1054.9 cm^{-1} band that is almost identical with the 1053.7 cm^{-1} band in solid nitrogen must be assigned to isolated MnN in the quintet state. Complexation by N_2 favors the triplet MnN state with a fundamental predicted to be 132 cm^{-1} higher by BPL/DFT calculations and the 1053.7−1054.9 cm^{-1} bands are assigned to $(NN)_xMnN$ in the triplet state. Here the electronic state of MnN is changed by the field of the complexing N_2 ligand(s) and not the matrix environment. We prefer to think of this reversal of low-lying MnN electronic states as a "ligand field effect" rather than a "matrix effect".

Note that the 916.1 cm^{-1} fundamental for ground state MnN is almost the same as the 938.0 cm^{-1} value for FeN, and both are higher than their monoxides,[8,25] MnN by 83 cm^{-1} and FeN by 65 cm^{-1}.

Gaussian 94 calculations with the BPL functional predict a triplet state MnN fundamental of 1022 cm^{-1} and bond length 1.529 Å and a quintet state lower by 0.8 kcal/mol with a 890 cm^{-1} fundamental and a 1.597 Å bond length. Similar calculations for the triplet NNMnN complex give a NN−MnN complex bond length of 1.898 Å and Mn−N frequency of 1030 cm^{-1}, and for the quintet complex the calculations give a longer complex bond length (2.041 Å) and lower Mn−N frequency (952 cm^{-1}). Clearly, complexing with N_2 blue-shifts the MnN fundamental frequency whereas the reverse is true for VN and TiN.[30] Of more importance, triplet MnN binds N_2 by 15.6 kcal/mol and quintet MnN binds N_2 by only 6.6 kcal/mol, based on BPL calculations, and ligation by N_2 accounts for the reversal of ground MnN electronic states.

As discussed for FeN, the VN, CrN, and MnN molecules are prepared here by reaction of the constituent atoms. The formation of N atoms in these experiments from dissociation of N_2 is evidenced by the presence of N_3 radical and the bright green luminescence from N atom recombination on sample annealing.[8]

Metal Dinitrides. In the iron/nitrogen matrix system, a sharp band at 903.6 cm^{-1} increased much more on annealing than the FeN band at 934.8 cm^{-1} and showed an intermediate mixed nitrogen isotopic band for two equivalent N atoms and a ^{54}Fe satellite appropriate for a single Fe atom species. Thus, the bent NFeN molecule was identified, and the valence angle (115 ± 5°) was calculated from isotopic frequencies; this observation was supported by DFT calculations, which predicted a triplet ground state with a 114° valence angle.[8]

Analogous but even more dramatic behavior was found in the chromium system. The sharp band at 875.7 cm^{-1} increases and then decreases in favor of the band at 883.3 cm^{-1}, which decreases on further annealing. Both bands exhibit 1/2/1 triplets with mixed isotopic nitrogen samples, which indicates that *two equivalent nitrogen atoms* are involved in the vibration. Several of these ^{52}Cr bands exhibit isotopic splittings for ^{53}Cr and ^{54}Cr present in natural abundance (^{52}Cr, 83.8%; ^{53}Cr, 9.6%; ^{54}Cr, 2.4%) with 36/4/1 relative intensities. This shows that a *single chromium atom* is involved in the vibration. The 14/15 ratios (1.0252, 1.0251) for these bands are lower than the diatomic value and appropriate for the ν_3 vibration of a bent NCrN molecule in two different matrix sites. The strong nitrogen isotopic triplets are slightly asymmetric: the $^{14}NCr^{15}N$ components are 1.7−1.8 cm^{-1} *below* the mean of the $^{14}NCr^{14}N$ and $^{15}NCr^{15}N$ values. This points to a higher symmetric stretching mode, and the weaker 956.1 and 963.8 cm^{-1} bands that track on annealing show the appropriate 14/15 ratios (1.0277, 1.0281) for the ν_1 mode in two different matrix sites. Furthermore, the weak 1/2/1 triplet patterns show the required (1.7−1.9 cm^{-1}) matching asymmetry with the mixed isotopic band *above* the mean of pure isotopic values. In a complementary relationship, the chromium 52/54 ratios are higher (1.002 52 for ^{14}N) than the diatomic value, which is in accord with the ν_3 vibration for NCrN.

The valence angle of NCrN can be calculated from the isotopic ν_3 frequencies.[8,24] For the first site, the 14/15 ratio gives a 113° upper limit and the 52/53 ratio a 109° lower limit; for the second site, 113° and 105° values are obtained. Hence, the valence angle of NCrN is accurately predicted at 109 ± 4°; the ±0.1 cm^{-1} frequency accuracy introduces only ±2° of error into this measurement.

Observation of the same 1/2/1 triplet absorptions with mechanical and statistical mixed isotopic nitrogen reagents and the strong growth on annealing show that NCrN is made from the N + CrN reaction.

The present DFT/BPL calculations found a stable $^3B_2$ state for NCrN with a 101° bond angle and ν_1 at 992 and ν_3 at 721 cm^{-1}. Although the agreement is not very good, the calculation offers some support for the assignment.

Similar DFT calculations predict that NVN and NMnN are also stable bent molecules. A weak sharp band at 820.1 cm^{-1} in the vanadium/nitrogen system increases on annealing, exhibits a triplet mixed isotopic spectrum and a 820.1/799.7 = 1.0252 ratio, which is appropriate for the antisymmetric stretching mode of a bent NVN molecule (109° valence angle upper limit). Likewise a weak 858.9 cm^{-1} band in the Mn experiments grows 3-fold on annealing, reveals a triplet mixed isotopic spectrum and a 858.9/838.4 = 1.0245 ratio, and is assigned to ν_3 of bent NMnN (127° valence angle upper limit).

It is interesting to note that there is much more NCrN and NFeN formed on annealing than NVN and NMnN, relative to the mononitride, in these experiments although calculations predict NVN and NMnN to be stable molecules. This is most likely due to competition between N_2 and N for reaction with the mononitride. Note that both VN and MnN are trapped only as the completely ligated $(NN)_xVN$ and $(NN)_xMnN$ species in pure nitrogen, but considerable CrN is trapped on surface sites in solid nitrogen along with NCrN. Hence, the complexation of N_2 with CrN is slow enough to allow N atoms to compete favorably for reaction with CrN to form NCrN in large yield, whereas VN and MnN react rapidly to form the dinitrogen complexes and only a small yield of the metal dinitride molecules.

Other Nitride Bands. Several bands in the tables noted with a question mark cannot be identified. Weak bands at 928.5 and 746.2 cm^{-1} in the vanadium experiments are appropriate for VN dimers and are tentatively assigned to VNVN and $(VN)_2$. It is difficult to identify the broader bands in the 830−750 cm^{-1} region.

The 822.7 and 778.8 cm^{-1} bands observed on deposition with Cr when CrN bands are strong, decrease (but not together) on annealing, and exhibit "diatomic CrN" and "dinitride NCrN" 14/15 ratios, respectively. These bands are tentatively assigned to CrN dimers with ring and chain structures, respectively. The 847.1 and the 829.6 cm^{-1} bands that appear on annealing give isotopic ratios appropriate for the NCrN triatomic molecule, and their relationship to the sharp NCrN bands suggests assignment to $(NN)_xCrN_2$ complexes. Finally, the sharp 685.9 and 690.8 cm^{-1} bands that also appear on annealing and show the same 14/15 ratios and sharp isotopic triplets as NCrN are probably also due to complexes of NCrN, but the shift from 883.3 and 875.7 cm^{-1} requires a stronger interaction. The $(N_2)CrN_2$ complex is suggested. Note that the lower bands show opposite asymmetry in the 14-Cr-15 component pointing to a lower frequency ν_1 mode in the complex.

Dinitrogen Complexes. Dinitrogen complexes with V, Cr, and Mn are related to the highly ligated complexes such as $Cr(CO)_6$, and the simple end-on and side-bonded complexes MNN and $M(N_2)$. The latter is particularly interesting as the N−N frequency is expected to be more reduced by the side-bonded interaction with a transition metal.

The present work is complementary to the study on chromium dinitrogen complexes by DeVore[21] and additional support is provided for the identification of $Cr(NN)_6$. In the present nitrogen matrix experiments, it is expected that energetic Cr atoms will form the stable, saturated dinitrogen complex. The mechanical mixture ($^{14}N_2 + {}^{15}N_2$) reveals a strong doublet with *four intermediate* mixed isotopic components, which is characteristic of the triply degenerate vibration (antisymmetric N−N) in octahedral symmetry[32] and confirms that the 2112 cm^{-1} band

is due to $Cr(NN)_6$. The 548.5 cm^{-1} band is also due to a Cr−NN deformation, stretching vibration. This band exhibits a very low 1.0169 isotopic 14/15 ratio, which shows that the metal is moving between (NN) subunits. The analogous $Cr(CO)_6$ molecule[33] has three infrared active f_u fundamentals: a very, very strong carbonyl stretching vibration at 2000 cm^{-1}, a very strong Cr−CO deformation at 668 cm^{-1}, and a strong Cr−CO stretching mode at 441 cm^{-1}. If the 548.5 cm^{-1} band corresponds to the 668 cm^{-1} band of $Cr(CO)_6$, then another $Cr(NN)_6$ fundamental is expected in the low 300 cm^{-1} region. Finally, it is interesting to note that the CO fundamental is red-shifted only 138 cm^{-1} in $Cr(CO)_6$ but the N_2 fundamental is red-shifted 215 cm^{-1} in $Cr(NN)_6$.

Three other weak bands are observed in the nitrogen matrix at 2192.4, 2156.3, and 2080.3 cm^{-1}; these bands exhibit 14/15 ratios for pure N−N stretching modes. Although the 2192.4 and 2080.3 cm^{-1} bands are near those assigned by DeVore to $Cr(NN)_5$, these bands do not track together on annealing. These bands are due to $Cr(NN)_x$ complexes with $x = 3$, 4, or 5, but we cannot determine which values are appropriate for each band. We do not have evidence for the identification of CrNN, but the recent observation[34] of CrCO at 1975 cm^{-1}, below the strongest $Cr(CO)_6$ band at 2000 cm^{-1}, and the present DFT calculations, cast doubt on DeVore's assignment of a 2215 cm^{-1} band to the end-bonded CrNN complex.

The end-bonded dinitrogen complex region for V in solid nitrogen contains several bands and some conclusions can be drawn. The sharp resolved pentet band system beginning at 562.8 cm^{-1} in the $^{14}N_2 + {}^{15}N_2$ experiment indicates a nondegenerate mode involving four N_2 subunits that are equivalent; the low 14/15 ratio shows that V is vibrating between N_2 subunits. A T_d structure must be ruled out because the nondegenerate stretching mode is not infrared active; however, a D_{2d} structure for $V(NN)_4$ has e and b_2 ligand stretching modes. The b_2 mode is expected to be strong and compatible with these observations. The sharp 2046.3 cm^{-1} band has the same annealing behavior and is appropriate for an e (degenerate) N−N stretching mode as the $^{14}N_2 + {}^{15}N_2$ experiment shows the pure isotopic components and no strong intermediate isotopic bands. Hence, we present evidence for $V(NN)_4$ with end-bonded ligands in a D_{2d} structure.

The sharp 2137.7 cm^{-1} band and its associated intermolecular mode at 455.6 cm^{-1} grow markedly on annealing and are the dominant features in both regions. Therefore these bands are probably due to $V(NN)_6$ analogous to $V(CO)_6$.[35] The 455.6 cm^{-1} band gives a sharp, resolved 1/2/1 triplet in the $^{14}N_2 + {}^{15}N_2$ experiment, revealing the coupling of two equivalent N_2 subunits in this mode. The 2137.7 cm^{-1} band reveals a strong doublet in the mixed isotopic experiment with weak intermediate bands consistent with a degenerate motion, but the spectrum is not as clean as shown in Figure 3 for $Cr(NN)_6$. The 455.6, 450.6, 445.0 cm^{-1} triplet for $V(NN)_6$ is, however, better resolved than this band for $Cr(NN)_6$. This assignment to $V(NN)_6$ is in disagreement with Huber et al.,[22] who assigned the strongest band on deposition to the completely ligated species. However, the present experiments suggest that annealing is required for complete ligation of vanadium to occur, in contrast to chromium, and that $V(NN)_6$ increases markedly on annealing at the expense of lower $V(NN)_x$ species. We see little possibility that the weaker bands assigned previously[22] to $V_2(NN)_{12}$, which show different annealing behaviors, are correctly identified.

With V and 0.5% N_2 in argon the strongest bands are 1945.0 and 1709.1 cm^{-1}. These bands give doublets with the mechanical mixture and a quartet and triplet with the statistical ($^{14,15}N_2$) mixture, which suggests assignment to VNN and $V(N_2)$. The DFT calculations support, but cannot confirm, these assignments. Figure 1 shows four more major bands between the $V(NN)_6$ and VNN frequencies that evolve on sequential annealing, namely, 1969.7, 2039.0, 2078.2, and 2098.9 cm^{-1}. The sextet nature of the 1969.7 cm^{-1} band with $^{14,15}N_2$ is in accord with $V(NN)_2$ identification. A straightforward but by no means definitive assignment of the latter three bands is $V(NN)_x$ ($x = 3$, 4, 5).

Laser-ablated Mn atoms in solid nitrogen give rise to two strong bands at 2103.5, 2100.4 cm^{-1} and at 452.5, 499.6 cm^{-1}, which increase 10% on annealing, and bands at 2199.7, 2116.9, and 2080.1 cm^{-1}, which grow 50% on annealing. In contrast to $Cr(CO)_6$, the stable manganese carbonyl is the binuclear $Mn_2(CO)_{10}$ molecule.[36,38] Assignment of the strong bands near 2100 cm^{-1} to the completely ligated Mn species requires $Mn(NN)_5$ to find a partner. From comparison of the strongest band in the spectrum of $Mn_2(CO)_{10}$ (2013 cm^{-1}) with that in the spectrum of $Cr(CO)_6$, the strong 2103.5, 2100.4 cm^{-1} bands are near the 2112 cm^{-1} $Cr(NN)_6$ band and are appropriate for $Mn(NN)_5$ or $Mn_2(NN)_{10}$, but it is not straightforward to determine which. The 14/15 ratios (Table 2) are appropriate for N−N stretching modes, but the intermediate bands in the $^{14}N_2 + {}^{15}N_2$ spectrum cannot identify the stoichiometry. The low-frequency bands 452.5, 442.4 cm^{-1} have very low 14/15 ratios as is appropriate for a mixed NN ligand deformation, stretching mode, but again the absorber cannot be identified. We prefer assignment of the strongest 2103.5, 2100.4 cm^{-1} and 452.5, 442.4 cm^{-1} bands to $Mn(NN)_5$ and the weaker set that grows more on annealing to the dimer $Mn_2(NN)_6$. The appearance of weaker bands, 2199.7 and 2080.1 cm^{-1}, around the stronger 2116.9 cm^{-1} band follows the pattern for $Mn_2(CO)_{10}$. The 2110 cm^{-1} shoulder and 508.5 cm^{-1} band are due to a smaller complex that reacts further on annealing to give the above higher complexes.

All three of these metals in pure nitrogen give bands near 1800 cm^{-1} that show pure N−N nitrogen isotopic ratios and doublets with $^{14}N_2 + {}^{15}N_2$. A similar band was found at 1801 in the Ti/N_2 system.[30] A $^{14,15}N_2$ sample was examined only for Cr, and the 1/2/1 triplet isotopic pattern was observed. These bands show a substantial (533−476 cm^{-1}) red shift from the N_2 fundamental and are assigned to the side-bonded complexes $M(N_2)$. These bands all decrease on annealing. In the V experiments, the 1851.6 cm^{-1} band gives way to 1861.9 and 1874.7 cm^{-1} bands, which are presumably due to higher $(NN)_xV(N_2)$ complexes. In the Cr experiments, the 1795.1 cm^{-1} band decreases in favor of a sharp 1803.5 cm^{-1} band. In the Mn experiments the 1844.2 cm^{-1} band decreases slightly on annealing and no other bands appear. It must be assumed that these $M(N_2)$ complexes have dinitrogen ligands attached, i.e., $(NN)_xM(N_2)$.

These metals give different results with N_2 in excess argon. For V, the 1709.1 cm^{-1} band that can be reasonably identified as $V(N_2)$ is replaced on annealing by a broader 1641.4 cm^{-1} band. If the 1851.6 cm^{-1} band is due to $(NN)_xV(N_2)$, then the 1641.4 cm^{-1} band is probably due to $(V_2)(N_2)$. Similar behavior was found for iron where the 1826.8 cm^{-1} band was replaced by a 1683.0 cm^{-1} band on annealing.[8] For Cr, no such bands were produced on sample deposition but annealing gave a band at 1613.7 cm^{-1}, which likewise could be due to a $(Cr_2)(N_2)$ species, but this identification must be considered tentative. For Mn, a 1819.3 cm^{-1} band behaved appropriately for $Mn(N_2)$. Taken together, there is considerable matrix spectroscopic evidence that V, Cr, Mn, and Fe form sideways-bonded $M(N_2)$ complexes that absorb in the 1900−1700 cm^{-1} region and exhibit substantial reduction of dinitrogen.

Conclusions

Laser-ablated V, Cr, and Mn atoms have been codeposited with Ar/N_2 mixtures and pure nitrogen for the purpose of preparing and trapping the elusive VN, CrN, and MnN molecules. The spectra are complicated by dinitrogen ligand complexes with both metal atoms and metal mononitrides. Careful annealing experiments have allowed the identification of isolated VN, CrN, and MnN in solid argon at 1026.2, 1044.3, and 916.1 cm^{-1} and bands for the $(NN)_xMN$ complexes in solid argon and nitrogen using nitrogen-15 substitution as a characteristic of the M−N vibration. The argon matrix VN fundamental is in reasonable agreement with the approximate 1020 $\pm$ 5 cm^{-1} gas-phase value; there are no gas-phase observations of CrN and MnN to date.

The bent NCrN molecule gives a particularly impressive spectrum with $\nu_3 = 875.7$ and $\nu_1 = 956.1$ cm^{-1}, 1/2/1 mixed nitrogen isotopic triplets, and natural ^{52}Cr, ^{53}Cr, ^{54}Cr isotopic splittings on the strong ν_3 bands. The valence angle is calculated at 109 $\pm$ 4° from this isotopic data.

The metal mononitride molecules are formed here by combination of metal and nitrogen atoms. The formation of N atoms by dissociation of N_2 is verified by the presence of N_3 radical and the bright green luminescence from N atom recombination on sample annealing. The NCrN molecule is formed by the N + CrN reaction.

In addition to bands in the 2200−1900 cm^{-1} region that are due to end-bonded $M(NN)_x$ complexes, weaker bands are observed in the 1900−1700 cm^{-1} region that exhibit nitrogen-15 shifts for N−N stretching modes and are assigned to side-bonded $M(N_2)$ complexes. These complexes exhibit substantial reduction of the dinitrogen fundamental frequency.

Acknowledgment. We appreciate financial support for this research from the University of Virginia and the Air Force Office of Scientific Research.

References and Notes

(1) Rawers, J.; Grujicic, M. *Mater. Sci. Eng.* **1996**, *207*, 188.
(2) Vanderschaeve, F.; Taillord, R.; Foct, J. *J. Mater. Sci.* **1995**, *30*, 6035.
(3) Wu, W. P.; Janke, D. *Ironmaking Steelmaking* **1996**, *23*, 247.
(4) Arai, T. *Am. Mach.* **1995**, *139*, 37.
(5) Ramanathan, S.; Oyama, S. T. *J. Phys. Chem.* **1995**, *99*, 16365.
(6) Douglas, A. E.; Veillette, P. J. *J. Chem. Phys.* **1980**, *72*, 5378.
(7) Simard, B.; Masoni, C.; Hackett, P. *J. Mol. Spectrosc.* **1989**, *136*, 44. Peter, S. L.; Dunn, T. M. *J. Chem. Phys.* **1989**, *90*, 5333.
(8) Chertihin, G. V.; Andrews, L.; Neurock, M. *J. Phys. Chem.* **1996**, *100*, 14609.
(9) Andrews, L.; Citra A.; Chertihin, G. V.; Neurock, M. Manuscript in preparation.
(10) Kunze, K. L.; Harrison, J. F. *J. Am. Chem. Soc.* **1990**, *112*, 3812.
(11) Harrison, J. F. *J. Phys. Chem.* **1996**, *100*, 3513.
(12) Huber, K. P.; Herzberg, G. *Constants of Diatomic Molecules*; Van Nostrand Reinhold: New York, 1979.
(13) Athénour, C.; Fémênias, J.-L.; Dunn. T. M. *Can. J. Phys.* **1982**, *60*, 109.
(14) Bauschlicher, C. W., Jr. *Chem. Phys. Lett.* **1983**, *100*, 515.
(15) Simard, B.; Niki, H.; Hackett, P. A. *J. Chem. Phys.* **1990**, *92*, 7012.
(16) Fletcher, D. A.; Scurlock, C. T.; Jung, K. Y.; Steimle, T. C. *J. Chem. Phys.* **1993**, *99*, 4288.
(17) Brabaharan, K.; Coxon, J. A.; Yamashita, A. B. *Can. J. Phys.* **1985**, *63*, 997.
(18) Mattar, S. M. *J. Phys. Chem.* **1993**, *97*, 3171.
(19) Gingrich, R. A. *J. Chem. Phys.* **1968**, *49*, 19.
(20) Burdett, J. K.; Graham, M. A.; Turner, J. J. *J. Chem. Soc., Dalton Trans.* **1972**, 1620.
(21) DeVore, T. C. *Inorg. Chem.* **1976**, *15*, 1315.
(22) Huber, H.; Ford, T. A.; Klotzbücher, W.; Ozin, G. A. *J. Am. Chem. Soc.* **1976**, *98*, 3176.
(23) Chertihin, G. V.; Bare, W. D.; Andrews, L. *J. Phys. Chem. A* **1997**, *101*, 5090.
(24) Chertihin, G. V.; Bare, W. D.; Andrews, L. *J. Chem. Phys.* **1997**, *107*, 2798.
(25) Chertihin, G. V.; Andrews, L. *J. Phys. Chem. A*, in press.
(26) Tiam, R.; Facelli, J. C.; Michl, J. *J. Phys. Chem.* **1988**, *92*, 4073. Hassanzadeh, P.; Andrews, L. *J. Phys. Chem.* **1992**, *96*, 9177.
(27) Frisch, M. J.; Trucks, G. W.; Schlegel, H. B.; Gill, P. M. W.; Johnson, B. G.; Robb, M. A.; Cheeseman, J. R.; Keith, T.; Petersson, G. A.; Montgomery, J. A.; Raghavachari, K.; Al-Laham, M. A.; Zakrzewski, V. G.; Ortiz, J. V.; Foresman, J. B.; Cioslowski, J.; Stefanov, B. B.; Nanayakkara, A.; Challacombe, M.; Peng, C. Y.; Ayala, P. Y.; Chen, W.; Wong, M. W.; Andres, J. L.; Replogle, E. S.; Gomperts, R.; Martin, R. L.; Fox, D. J.; Binkley, J. S.; Defrees, D. J.; Baker, J.; Stewart, J. P.; Head-Gordon, M.; Gonzalez, C.; Pople J. A. *Gaussian 94, Revision B.1*; Gaussian, Inc.: Pittsburgh, PA, 1995.
(28) Mattar, S. M.; Doleman, B. J. *Chem. Phys. Lett.* **1993**, *216*, 369.
(29) Martinez, A.; Köstner, A. M.; Salahub, O. R. *J. Phys. Chem. A* **1997**, *101*, 1532. Pyykkö, P.; Tamm, T. *J. Phys. Chem. A.*, in press.
(30) Kushto, G. P.; Souter, P. F.; Chertihin, G. V.; Andrews, L. Manuscript in preparation.
(31) Chertihin, G. V.; Andrews, L. *J. Phys. Chem.* **1995**, *99*, 6356.
(32) Darling, J. H.; Ogden, J. S. *J. Chem. Soc., Dalton Trans.* **1972**, 2496.
(33) Jones, L. H.; McDowell, R. S.; Goldblatt, M. *Inorg. Chem.* **1969**, *8*, 2349.
(34) Souter, P. F.; Andrews, L., *J. Am. Chem. Soc.* **1997**, *119*, 7350.
(35) Hanlan, L.; Huber, H.; Ozin, G. A. *Inorg. Chem.* **1976**, *15*, 2592.
(36) Levenson, R. A.; Gray, H. B.; Ceaser, G. P. *J. Am. Chem. Soc.* **1970**, *92*, 3653.
(37) Flitcroft, N.; Huggins, D. K.; Kaesz, H. D. *Inorg. Chem.* **1964**, *3*, 1123.
(38) Kundig, E. P.; Moskovits, M.; Ozin, G. A. *Angew. Chem., Int. Ed. Engl.* **1975**, *14*, 292.